



Interactions between iron mineral-humic complexes and hexavalent chromium and the corresponding bio-effects[☆]

Zhiyong Zheng^{a, c, 1}, Yue Zheng^{a, b, 1}, Xiaochun Tian^d, Zhaohui Yang^c, Yanxia Jiang^d, Feng Zhao^{a, *}

^a CAS Key Laboratory of Urban Pollutant Conversion, Institute of Urban Environment, Chinese Academy of Sciences, 361021 Xiamen, China

^b University of Chinese Academy of Sciences, Beijing, 100049, China

^c College of Environmental Science and Engineering, Hunan University, 410082 Changsha, China

^d State Key Laboratory of Physical Chemistry of Solid Surfaces, Department of Chemistry, College of Chemistry and Chemical Engineering, Xiamen University, 361021 Xiamen, China

ARTICLE INFO

Article history:

Received 26 February 2018

Received in revised form

16 May 2018

Accepted 17 May 2018

Available online 26 May 2018

Keywords:

Chromium

Humic substance

Iron mineral

Microbial diversity

Adsorption

ABSTRACT

The interfacial behaviors of chromium are fundamental for understanding the environmental effects of chromium in contaminated environments. However, complex surfaces can cause chromium to exhibit a variety of behaviors, especially when humic substances are considered. This work illustrated the role of humics (humic acid and fulvic acid) during the adsorption of Cr(VI) onto iron minerals (magnetite and hematite). The interfacial behaviors were investigated through their adsorption kinetics, adsorption isotherms, and thermodynamics. Then, the microbial diversity was monitored to reflect the bio-effects of Cr(VI) adsorbed onto four iron oxide-humic complexes. The differences in the adsorption capacities and mechanisms of Cr(VI) on the surfaces of the iron mineral-humic complexes were observed. Humics obviously decreased the adsorption capacities of Cr(VI) on the hematite complexes and relieved the decline in the microbial diversity; meanwhile, humics imposed relatively insignificant changes to the Cr(VI) adsorption capacity onto the magnetite complexes. Thus, the corresponding microbial diversity might be mainly affected by released micelles formed by Cr(VI) and humics. These results illustrate the complexities of the interfacial behaviors of Cr(VI) on the surfaces of iron mineral-humic complexes and broaden the current understanding of chromium migration and transportation.

© 2018 Elsevier Ltd. All rights reserved.

1. Introduction

Chromium-contaminated soils have long been considered as an environmental problem (Kazakis et al., 2018; Brose and James, 2013). Moreover, based on a sampling survey, the ratio of contaminated soil is still increasing (MLR, 2014). The migration, transformation, and bioavailability behaviors of chromium are dominated by interactions at the solid-fluid interface, especially along the interfaces of iron oxides (Zachara et al., 1987). Although the interfacial reactions would be decided by multiple reasons including environmental conditions (pH, ionic strength, and temperature, etc.) and interfacial properties. This work only focuses on

interfaces of iron mineral-humic complexes by controlling environmental parameters. The changes of interfacial reactions can alter the pathways and kinetics, and consequently result in chromium exhibiting distinct bio-effects. For example, Cr(VI) is mainly reduced to Cr(III) and chelated by hydroxy groups on the surface of Fe(II) (Kendelewicz et al., 2000; Grossl et al., 1997), while the adsorption of Cr(VI) by Fe(III) is mainly achieved by ion exchange between hydroxy and Cr(VI) (Cao et al., 2012). Although some studies have been reported on this topic, more complex mineral interfaces are expected to be critical and predominant in different environments (Batchelli et al., 2010; Hiraide, 1992; Tipping et al., 2002).

Humic substances are heterogeneous and functional group-rich organic molecules (Lovley et al., 1996) that account for 60% of the overall dissolved organic carbon in aquatic systems (Stevenson, 1994). When humics interact with minerals, negatively charged humics are likely to be retained on positively charged mineral surfaces. Thus, the interactions between humics and minerals could

[☆] This paper has been recommended for acceptance by B. Nowack.

* Corresponding author.

E-mail address: fzhao@iue.ac.cn (F. Zhao).

¹ Equal contribution as co-first authors.

alter the original properties of either substance and generate complex humic minerals (Hu et al., 2010). For example, magnetite that is coated with humic acid could prevent the transformation of the mineral core during an interaction with Cr(VI) (Jiang et al., 2014). Nevertheless, it is worth mentioning that complicated humics include both soluble humic acid and fulvic acid (Hiraide, 1992). Meanwhile, the minerals that can interact with humics encompass various structures with different properties. Hence, it is necessary to systematically study the performances of chromium on the interfaces of various humic minerals with different properties rather than focus on only one model interface.

Shifts in microbial communities are mainly influenced by environmental pollution within contaminated soils (Nannipieri et al., 2003). Microbial processes link the fluxes of cyclic elements and drive the cycles of multiple nutrients. Therefore, the microbial diversity, which represents one of the key parameters of microbial communities, could be used to reflect the bio-effects of heavy metal pollution (Brookes, 1995). Meanwhile, the bio-effects of Cr(VI) are determined by multiple factors, including interfacial adsorption and released micelles. Humics may favor the toxic persistence of Cr(VI) relative to microbial communities because humics can form micelles with Cr(VI) (Leita et al., 2009). In this work, we focus on the interactions between humics and Cr(VI) and address the role of interfacial adsorption on the bio-effects of chromium.

In this study, the interactions between various iron mineral-humic complexes and Cr(VI) were systematically studied by investigating two minerals, namely, magnetite and hematite, and two humics, namely, humic acid and fulvic acid. Four complexes, including magnetite-humic acid (Mag-HA), magnetite-fulvic acid (Mag-FA), hematite-humic acid (Hem-HA) and hematite-fulvic acid (Hem-FA), were applied to explore their interactions with Cr(VI), each of which was deeply explored with regard to their adsorption kinetics, isotherms, and thermodynamics. From the perspective of bio-effects, the four complexes were added into soil after being coated with Cr(VI) to investigate the shifts in microbial diversity. This work could provide comprehensive insight into how humics change the interfacial behaviors of Cr(VI) and the resulting bio-effects.

2. Experimental methods

Synthesis of iron minerals. Magnetite (Mag) was synthesized using a modified hydrothermal method (Liu et al., 2008). In brief, 3.66 g of FeCl₃ and 4.20 g of FeSO₄ were dissolved in 100 mL MilliQ water (Millipore Corporation, Billerica, MA, USA), after which the solution was heated to 90 °C before the addition of 10 mL of NH₄OH (25%). The mixture was kept at 90 °C, stirred for half an hour, and cooled to the ambient temperature. Subsequently, the black precipitates were gathered and washed until the pH of the supernatant was neutral. Hematite (Hem) was also synthesized using the hydrothermal method. In brief, 50 mL of FeCl₃ solution (1 M) was added one drop at a time into 450 mL of boiling MilliQ water, following which the solution turned from golden brown to dark red. After adding the final drop, the solution was heated for 5 min. Then, the solution was cooled to the ambient temperature and dialyzed for approximately 48 h in a solution of HClO₄ (pH 3.5) (Mulvaney et al., 1988). The methods employed for the structural characterization are described in the Supporting Information.

Preparation of the iron mineral-humic complexes. The iron mineral-humic complexes were obtained by absorbing excess humic acid or fulvic acid onto magnetite or hematite (Iglesias et al., 2010). In brief, humic acid was dissolved in a 20 mM NaCl solution before its pH value was adjusted to 7 using a 5% (w/w) HCl or NaOH solution, thereby forming a 600 mg L⁻¹ humic acid solution. Then, 200 mg of either magnetite or hematite was added to a 1 L

flask containing a 250 mL humic acid solution. The flask was shaken at 150 rpm at a temperature of 298 K in the dark for 24 h. The mixture was then centrifuged at a speed of 7800 rpm for 10 min, after which the precipitates were collected and washed three times. The Mag-HA or Hem-HA complexes were obtained after the precipitates were freeze-dried. Except for the replacement of humic acid with fulvic acid, the Mag-FA and Hem-FA complexes were prepared similarly.

Procedure of Cr(VI) adsorption. All of the Cr(VI) adsorption batch experiments were accomplished in 50 mL flasks within temperature-controlled shaking incubator at a speed of 150 rpm. The Cr(VI) solution was obtained by dissolving K₂Cr₂O₇ into 20 mM of NaCl, and the pH value of the solution was altered to neutral using a 5% (w/w) HCl or NaOH solution. After cultivation, the samples were taken from the flasks using syringes and were subsequently filtered using 0.22 μm filters.

To derive their kinetic curves, 15 mg of each mineral complex (i.e., Mag, Mag-HA, Mag-FA, Hem, Hem-HA, and Hem-FA) was added to a 10 mL Cr(VI) solution with concentrations of 5, 8 or 10 mg L⁻¹, after which the mixtures were sampled at fixed time intervals. The adsorption isotherms were carried out at 298 K, 308 K, and 318 K. In all, 20 mg of Mag, 20 mg of the Mag-HA, Mag-FA, Hem-HA, and Hem-FA complexes, and 10 mg of Hem were added to 10 mL Cr(VI) solutions with concentrations varying from 2 to 26 mg L⁻¹ (2–30 mg L⁻¹ for Mag-FA), after which samples were taken after 24-h cultures. The Cr(VI) complexes obtained under 298 K were collected for biological experiments. The initial and residual Cr(VI) were both analyzed at 540 nm using an ultraviolet–visible (UV–Vis) spectrophotometer (UV-1200, Mapada, China) (Yang et al., 2014). The quantities of Cr(VI) adsorbed onto the iron oxides or iron oxide complexes were calculated using the following equation:

$$q_e = \frac{C_0 - C_e}{m} V \quad (1)$$

where q_e is the Cr(VI) adsorption capacity at adsorption equilibrium (mg g⁻¹), C_0 and C_e are the initial concentration and equilibrium concentration of Cr(VI) in the solution (mg L⁻¹), respectively, V is the volume of the Cr(VI) solution (L) and m is the weight of the iron oxide or iron oxide complex (mg).

Soil microcosms of iron oxides and iron oxide-humic complexes. Soil samples (at depths of 5–20 cm) were collected from a paddy field located in Xiamen (Fujian, China, 24°37'18"N, 118°2'34"E). To minimize spatial disparities, approximately 4 kg of soil was mixed to form homogeneous samples prior to the experiments. Twelve soil microcosms with volumes of 60 mL were mixed with different mineral complexes (i.e., Mag, Mag-HA, Mag-FA, Hem, Hem-HA, and Hem-FA) either with or without Cr(VI) in sealed bottles. The ratio of soil was regulated at 18% to maximize microbe activity (Ge et al., 2011), and the exposure dosage of each mineral complex was 1‰. The microcosms were incubated at 25 °C in the dark, and samples were taken after 10 and 20 days. The batch experimental design engendered 72 microcosms with 3 duplicates per exposure dosage.

Soil DNA extraction and bacterial community analysis. Each soil sample was entirely mixed, and the extraction and purification of genomic DNA were conducted following a previous report (Yang et al., 2007). The methods employed for the quantification and sequencing of the purified genomic DNA were described in a previous paper (Zheng et al., 2014a). In brief, the genomic DNA was polymerase chain reaction (PCR) amplified to obtain the V4-V5 region, after which the PCR products were purified before constructing libraries for Illumina MiSeq sequencing. The sequenced data were processed using the Quantitative Insights Into Microbial

Ecology (QIIME version 1.9) pipeline. The diversity of the bacterial community in each soil sample was evaluated using two indexes, namely, the observed species and Chao1.

3. Results and discussion

Structural characterization of the mineral-humic complexes.

The functional groups of humic acid and fulvic acid were first characterized using Fourier-transform infrared spectroscopy (FTIR) (Fig. S1). The C-O functional groups at 1043 cm^{-1} shared by humic acid and fulvic acid can complex with the surfaces of both magnetite and hematite (Gu et al., 1994). Nonetheless, there is a large variety of functional groups (e.g., C=C and N-H) in fulvic acid that could present additional binding sites for adsorption (Table S1).

First, the two precursor iron oxides were observed through transmission electron microscopy (TEM), both of which were approximately 10 nm in diameter (Fig. S2). Then, the two iron oxides were identified via X-ray diffraction (XRD), the results of which revealed that they were consistent with expected iron minerals (Fig. S3), i.e., magnetite (Mag) and hematite (Hem). After humics were coated onto the minerals, the structural characterization of each mineral-humic complex (Mag-HA, Mag-FA, Hem-HA, and Hem-FA) was performed based on the crystal structure (via XRD), the surface area and pore size (via their N_2 adsorption-desorption isotherms), and the stability of the colloidal dispersion (via the zeta potential). The crystal forms of the original iron minerals coated with humics did not change (Fig. S3). As shown in Fig. 1AB, the N_2 adsorption-desorption isotherms of the minerals and mineral-humic complexes can be classified as type IV with an H2

hysteresis loop (Sing et al., 1985). Furthermore, based on the Brunauer-Emmett-Teller model, the specific surface areas of magnetite and hematite were 80.25 and $104.02\text{ m}^2\text{ g}^{-1}$, respectively. The humic acid coating decreased the total surface areas of the iron minerals, and the fulvic acid coating did the same to a greater extent. Even so, the absorption of Cr(VI) onto each mineral-humic complex was determined by examining multiple factors, including their specific surface areas and functional groups. As shown in Fig. 1CD, the pH values of the point of zero charge (pH_{ZPC}) of magnetite and hematite were 6.5 and 7.4 respectively, which are similar to the findings of previous investigations (Chang and Chen, 2005; He et al., 2008), while the pH_{ZPC} values of the mineral-humic complexes obviously decreased after being coated with humic acid and fulvic acid. That is, the humic acid and fulvic acid coatings similarly lowered the pH_{ZPC} values of magnetite and hematite (Fig. 1CD). A decline in the pH_{ZPC} value would increase the stability of an iron mineral-humic complexes and decrease the electrostatic attraction between Cr(VI) and a mineral surface (Zhang et al., 2017).

Interactions between the mineral-humic complexes and Cr(VI).

Compared with the original iron minerals, the iron mineral-humic complexes exhibited different surface performances based on the abovementioned structural characterization. To understand the interactions between the mineral-humic complexes and Cr(VI), we demonstrated the associated processes in detail from three perspectives: their adsorption kinetics, adsorption isotherms, and thermodynamics.

Adsorption kinetics. Since Cr(VI) is a heavy metal, its adsorption kinetics were investigated to confirm whether a pseudo-first-order model or a pseudo-second-order model would effectively fit the adsorption performances of Cr(VI) onto the various mineral-humic

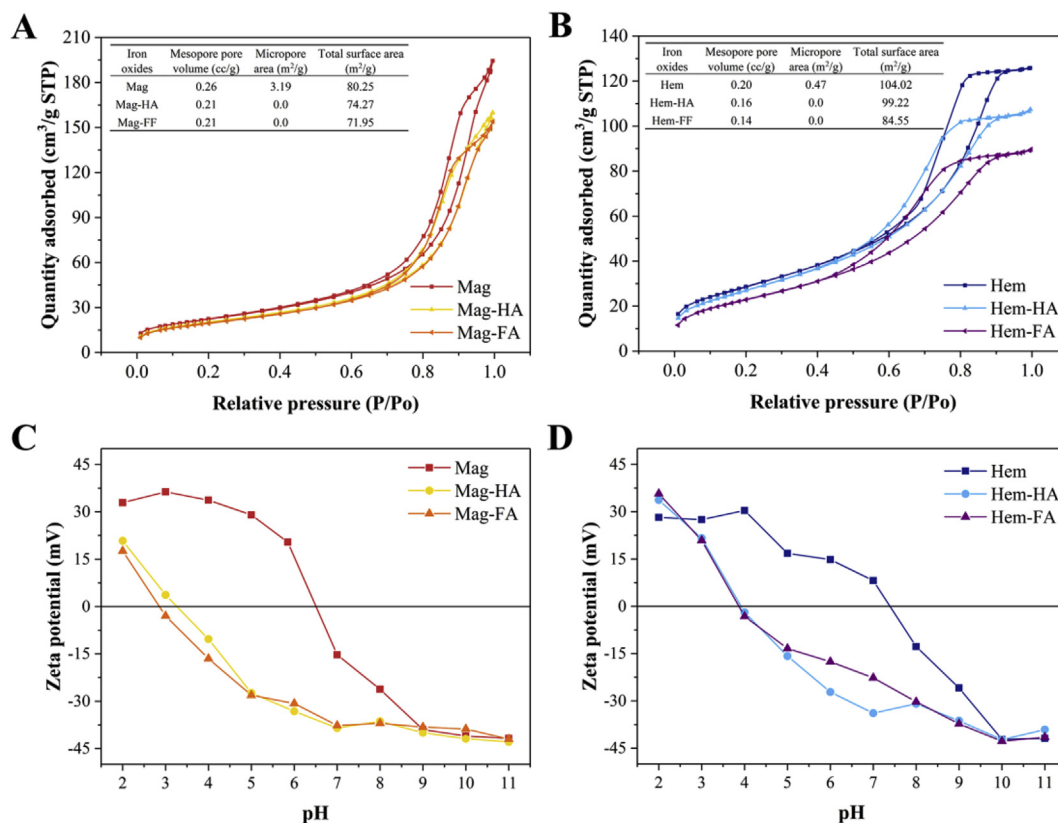


Fig. 1. The N_2 adsorption-desorption isotherms of the magnetite group (A) and hematite group (B) and the zeta potentials of the magnetite group (C) and hematite group (D) (Mag: magnetite; Mag-HA: magnetite-humic acid complex; Mag-FA: magnetite-fulvic acid complex; Hem: hematite; Hem-HA: hematite-humic acid complex; Hem-FA: hematite-fulvic acid complex).

complexes. Detailed information regarding both the pseudo-first-order model and the pseudo-second-order model are available in the Supporting Information. The pseudo-second-order model demonstrated a better fit (Fig. 2) with a high correlation coefficient ($R^2 \geq 0.992$) than the pseudo-first-order model (Table S2 and Table S3). Accordingly, the pseudo-second-order model better reflected chemical adsorption processes involving valence forces through the sharing or exchange of electrons (Qiu et al., 2009).

According to the reflection characteristics observed during X-ray photoelectron spectroscopy (XPS) of the chemical adsorption (Fig. S4ABC and Fig. S4EF), Cr(VI) and Cr(III) coexisted on all of the surface types except that of hematite, because the Fe(II) components of magnetite and humics within mineral-humic complexes can trigger the reduction of Cr(VI) to Cr(III) (Jiang et al., 2014). Compared with the adsorption of Cr(VI) by magnetite and by the mineral-humic complexes, the adsorption of Cr(VI) by hematite may be primarily related to the ion exchange of hydroxy groups on the surfaces of hematite and Cr(VI) (Cao et al., 2012). Thus, no Cr(III) was detected in the XPS spectra (Fig. S4D).

Adsorption isotherms. The quantities of Cr(VI) (q_{\max}) adsorbed onto the iron minerals and iron mineral-humic complexes were analyzed under three different temperatures at equilibrium (Fig. 3). For the magnetite complexes, the q_{\max} of both Mag-HA and Mag-FA rose with an increase in the temperature, but the q_{\max} of Mag showed an opposite trend. For the hematite complexes, the q_{\max} of Hem and Hem-HA decreased with an increase in the temperature, while the q_{\max} of Hem-FA increased with an increasing

	Mag	Mag-HA	Mag-FA	Hem	Hem-HA	Hem-FA
q_{\max} 298 K	3.42	1.77	3.96	7.94	3.98	4.51
	2.76	1.91	4.58	7.08	3.71	4.97
	2.20	2.16	5.73	6.10	3.38	5.43
K_L 298 K	1.25	0.85	2.51	2.66	0.72	1.29
	1.94	1.89	5.21	2.82	0.70	1.79
	5.67	4.23	9.66	3.38	0.63	3.85
K_F 298 K	1.35	1.01	1.57	2.09	1.27	1.48
	1.32	1.11	1.76	2.02	1.22	1.57
	1.30	1.25	1.97	1.93	1.16	1.82

Fig. 3. The maximum sorption capacity (q_{\max}), Langmuir constant (K_L) and Freundlich constant (K_F) of Cr(VI) onto different mineral surfaces at equilibrium (Mag: magnetite; Mag-HA: magnetite-humic acid complex; Mag-FA: magnetite-fulvic acid complex; Hem: hematite; Hem-HA: hematite-humic acid complex; Hem-FA: hematite-fulvic acid complex).

temperature. This indicates that the adsorption capacities of Cr(VI) onto Mag-HA, Mag-FA and Hem-FA are favorable at higher temperatures; meanwhile, the adsorption capacities of Cr(VI) onto

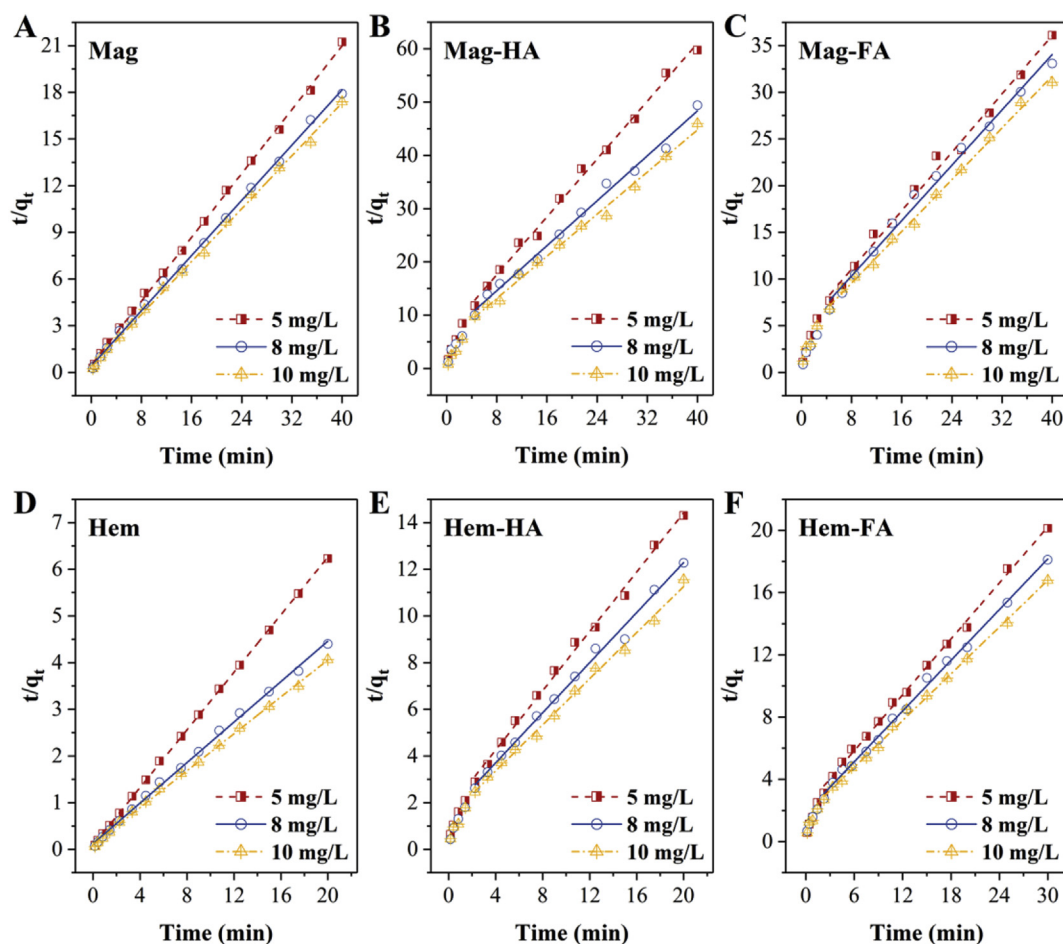


Fig. 2. Pseudo-second-order plots for Cr(VI) adsorption (Mag: magnetite; Mag-HA: magnetite-humic acid complex; Mag-FA: magnetite-fulvic acid complex; Hem: hematite; Hem-HA: hematite-humic acid complex; Hem-FA: hematite-fulvic acid complex).

magnetite, hematite, and Hem-HA are favorable at lower temperatures.

To further explore the adsorption isotherms, we constructed adsorption isotherm models according to four classic models (i.e., the Langmuir, Freundlich, Temkin, and Brunauere-Emmette-Teller models) based on the experimental data under different temperatures.

The Langmuir model shown in equation (2) (Wu et al., 2014) was fitted using the experimental data with a high correlation (Fig. S5, Table S4, and Table S5):

$$\frac{C_e}{q_e} = \frac{C_e}{q_{max}} + \frac{1}{q_{max}K_L} \quad (2)$$

where C_e is the equilibrium concentration of Cr(VI) (mg L^{-1}), q_e is the quantity of Cr(VI) adsorbed at equilibrium (mg g^{-1}), q_{max} is the maximum adsorption capacity of Cr(VI) corresponding to a full monolayer coverage (mg g^{-1}), and K_L is the Langmuir constant (L mg^{-1}), which is the ratio of the adsorption/desorption rates associated with the energy of adsorption.

Based on the Langmuir model, the range of R_L values was concentrated between 0.003 and 0.058 (Table S4 and Table S5), suggesting that Cr(VI) was prone to adsorb onto the surfaces discussed in this study (Nethaji et al., 2013). As shown in Tables S4–S5, the coating of humic acid onto either magnetite or hematite resulted in minimum K_L values among the corresponding minerals. This suggests that the binding energies between Cr(VI) and the mineral-humic acid complexes were lower than those between Cr(VI) and the minerals and mineral-fulvic acid complexes (Tang et al., 2014). It is therefore reasonable to assume that the binding energies between Cr(VI) and the humic acid molecules are weaker than those between Cr(VI) and the fulvic acid molecules and the magnetite and hematite sites. Such loose binding energies may cause the release of adsorbed Cr(VI) into the environment, further disrupting the microbial ecology.

The Freundlich adsorption isotherm is also presented mathematically in equation (3) (Freundlich, 1906), and the fitting plot as well as the corresponding parameters are presented at Fig. S6, Table S6, and Table S7:

$$\ln q_e = \ln K_F + \frac{1}{n} \ln C_e \quad (3)$$

where K_F is a Freundlich constant associated with the adsorption capacity (L g^{-1}), and $1/n$ is an empirical parameter demonstrating the favorability of the adsorption process. A straight line was obtained when $\ln q_e$ was plotted against C_e (Fig. S6); these two parameters were calculated from the intercept and slope of the corresponding plot (Table S9 and Table S10).

According to the Freundlich model, we also concluded that the adsorption of Cr(VI) was favorable on all of the surfaces because all of the $1/n$ values were far less than 1 (Table S6 and Table S7) (Wu et al., 2014). The q_{max} values derived from the Langmuir model and the K_F values from the Freundlich model both reflect the adsorption capacity, and they exhibited identical tendencies (Tables S4–S7). The adsorption capacities (i.e., q_{max} and K_F) of the Mag-HA and Hem-HA complexes were minimal among the four complexes based on magnetite and hematite, indicating that the coating of humic acid onto the mineral surfaces resulted in a relatively low Cr(VI) adsorption. Meanwhile, the adsorption capacity of Mag-FA was the highest among the magnetite complexes, and the adsorption capacity of hematite was the highest among the hematite complexes. These adsorption capacities reflected by q_{max} and K_F are also consistent with the quantities of Cr(VI) (q_e) adsorbed onto surfaces.

The Temkin model further assumes that the heat of adsorption of all adsorbate molecules in a layer would decline linearly rather than logarithmically (Aharoni and Ungarish, 1977). Moreover, the Brunauere-Emmette-Teller model states that Cr(VI) could be adsorbed onto the surfaces of mineral complexes to form multiple layers in a random distribution. Detailed information regarding the Temkin isotherm and Brunauere-Emmette-Teller isotherm models can be found in Figs. S7–8 and Tables S8–11.

Thermodynamics. To better understand how Cr(VI) was adsorbed onto the various mineral surfaces, three thermodynamic parameters, namely, the changes in the standard free energy (ΔG^0), enthalpy (ΔH^0), and entropy (ΔS^0), were calculated using equations (4)–(6) (Gupta et al., 2006):

$$\Delta G^0 = -RT \ln b \quad (4)$$

$$\Delta H^0 = R \frac{T_1 T_2}{T_1 - T_2} \ln \frac{b_1}{b_2} \quad (5)$$

$$\Delta S^0 = \frac{\Delta H^0 - \Delta G^0}{T} \quad (6)$$

where b is the Langmuir constant (the units of K_L should be altered into milligrams per gram to calculate ΔG^0) at a temperature T , and R is the universal gas constant.

Based on the resulting thermodynamic parameters (Fig. 4), the adsorption of Cr(VI) onto each mineral surface was spontaneous, which is justified by the positive values of ΔS^0 and the negative values of ΔG^0 (Niwas et al., 2000). Moreover, because all of the ΔG^0 values in this study ranged from -20 to -80 kJ mol^{-1} (Weng et al., 2009), the adsorption processes of Cr(VI) onto the mineral surfaces included both physisorption and chemisorption. Meanwhile, all of the ΔH^0 values for the mineral surfaces were positive except for that of Hem-HA, which was negative. Therefore, the adsorption of Cr(VI) onto Hem-HA was dominated by physisorption, since physisorption processes are exothermic (Huang and Wan, 2009). The adsorption processes could determine the adsorption stability. Normally, chemisorption is stronger than physisorption.

Mineral-humic complexes with Cr(VI) shifts in the microbial diversity. To evaluate how the mineral-humic complexes affected the microbial communities after binding with Cr(VI), this work investigated the shifts in the bio-diversity of the paddy soil samples with the addition of the mineral complexes (i.e., Mag-HA, Mag-FA, Hem-HA, and Hem-FA) with Cr across 20 days. The genomic DNA

		Mag	Mag-HA	Mag-FA	Hem	Hem-HA	Hem-FA
ΔG^0 (kJ/mol)	298 K	-34.79	-33.83	-36.51	-36.65	-33.42	-34.87
	308 K	-37.08	-37.01	-39.60	-38.03	-34.46	-36.87
	318 K	-41.11	-40.34	-42.52	-39.75	-35.29	-40.09
ΔS^0 (J/K·mol)	298 K	164.90	164.15	165.05	130.73	107.63	151.79
	308 K	166.99	169.11	169.74	130.97	107.52	153.36
	318 K	174.42	174.27	173.59	132.26	106.74	158.67
ΔH^0 (kJ/mol)		14.35	15.08	12.68	2.31	-1.34	10.37

Fig. 4. The changes in the standard free energy (ΔG^0), enthalpy (ΔH^0), and entropy (ΔS^0) of the adsorption of Cr(VI) onto the mineral surfaces (Mag: magnetite; Mag-HA: magnetite-humic acid complex; Mag-FA: magnetite-fulvic acid complex; Hem: hematite; Hem-HA: hematite-humic acid complex; and Hem-FA: hematite-fulvic acid complex).

was sampled and isolated on the 10th and 20th days for sequencing. The observed species and the Chao1 index were calculated at a sequencing depth of 38 900 reads per sample. These two indexes were used to compare and estimate the diversity of each microbial community (Zheng et al., 2014b). The trend of the observed species was consistent with the Chao1 index across all samples (Fig. 5). For the control groups without the addition of Cr, the coating of humic acid onto either magnetite or hematite increased the diversity index more than the coating of fulvic acid.

In contrast to the control groups, the microbial diversity indexes of the samples evidently decreased after adding the complexes with Cr. To facilitate a convenient comparison of the changes in the bio-diversity, AD was defined as the parameter reflecting the decrease in the bio-diversity in the minerals/complexes without Cr(VI) relative to the minerals/complexes with Cr(VI). For the samples with magnetite complexes, AD_{Mag} was approximately 1.5 times less than AD_{Mag-HA} and 2 times less than AD_{Mag-FA} because the micelles are capable of persisting the toxicity of Cr(VI) (Leita et al., 2009). Meanwhile, AD_{Hem} was the highest among the samples with hematite complexes since the largest amount of adsorbed chrome was accomplished in a hexavalent valence state. From the perspective of humic substances, Mag-HA and Mag-FA accelerated the decrease in bio-diversity among the magnetite complexes. However, when the same two types of humics participated with hematite, the drops of AD_{Hem-HA} and AD_{Hem-FA} were relieved because of the limited toxicity retention of Cr(VI) within micelles. Therefore, when humics are complexed with various iron minerals, different humics could play different roles in the shift of the bio-diversity. Even the addition of one humic substance changed the

bio-effects upon being complexed with different minerals.

The bio-effects of the mineral complexes with Cr(VI) resulted from multiple factors. Based on the above analysis of the interactions between the mineral-humic complexes and Cr(VI), adsorption isotherms can provide a quantification of the adsorption capacities of different mineral-humic complexes; meanwhile, an examination of the thermodynamics could provide a potential adsorption stability. A higher adsorption capacity and a smaller adsorption stability would lead to a greater decrease in the bio-diversity.

4. Conclusions

This work discussed the interfacial behaviors of Cr(VI) adsorbed onto the surfaces of iron mineral-humic complexes. Four types of iron mineral-humic complexes (Mag-HA, Mag-FA, Hem-HA, and Hem-FA) were constructed from two types of humics (i.e., humic acid and fulvic acid) and two types of minerals (i.e., magnetite and hematite). The interfacial behaviors were studied according to their adsorption kinetics, adsorption isotherms, and thermodynamics. All of the adsorption parameters were fitted well using a pseudo-second-order model, indicating that chemisorption played a substantial role. The adsorption capacities of Cr(VI) onto Mag-HA, Mag-FA, and Hem-FA were favored at higher temperatures, while those onto Mag, Hem, and Hem-HA were favored at lower temperatures. Moreover, humic acid molecules on iron minerals have weaker and smaller affinities to Cr(VI) than fulvic acid molecules based on the resulting Langmuir constants and Freundlich constants. A detailed thermodynamic study illustrated that chemisorption and

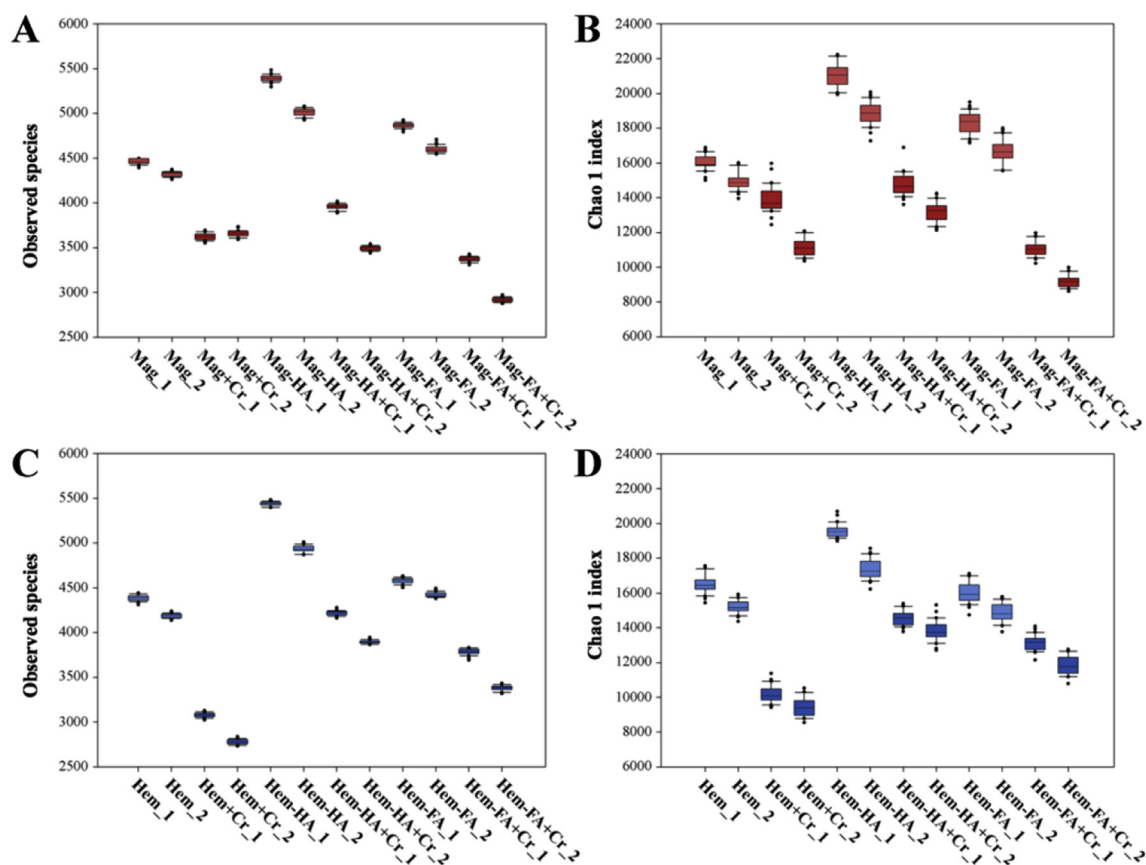


Fig. 5. Microbial diversity indexes of the paddy soil samples shifted by different mineral-humic complexes either with or without Cr (Mag: magnetite; Mag-HA: magnetite-humic acid complex; Mag-FA: magnetite-fulvic acid complex; Hem: hematite; Hem-HA: hematite-humic acid complex; Hem-FA: hematite-fulvic acid complex). The sample names labeled with Cr indicate the complexes bonded with Cr(VI). The microbial communities were sampled on the 10th and 20th days, which are suffixed with "1" and "2", respectively.

physorption coexisted in the adsorption of Cr(VI) onto both iron minerals and iron mineral-humic complexes. In addition, chemisorption was dominant for all iron minerals and iron mineral-humic complexes except for Hem-HA. In addition, the microbial diversity was monitored to reflect the bio-effects of Cr(VI) adsorbed onto iron mineral-humic complexes. The microbial diversity diminished noticeably after the addition of mineral complexes with Cr(VI). Humics obviously relieved the adsorption capacity of Cr(VI) onto the hematite complexes and reduced the decline in the microbial diversity. Nevertheless, humics were not able to significantly change the adsorption capacity of Cr(VI) onto the magnetite complexes, and thus, the corresponding microbial diversity might be mainly affected by the released micelles. These results illustrate the complexities associated with the interfacial behaviors of Cr(VI) on the surfaces of iron mineral-humic complexes and broaden the existing understanding of chromium migration and transportation.

Funding

This work was supported by the NSFC (21777155 and 41471260), the Xiamen Municipal Science and Technology Program (3502Z20172027) and the Fujian Province S&T Project (2016T3032).

Declarations of interest

None.

Appendix A. Supplementary data

Supplementary Material. Experimental materials and methods, supplementary test, FTIR spectroscopy, SEM images, XRD patterns, XPS spectrum, adsorption kinetics parameters, langmuir isotherm parameters, freundlich plots, freundlich isotherm parameters, temkin plots, temkin isotherm parameters, BET plots, BET isotherm parameters.

Supplementary data related to this article can be found at <https://doi.org/10.1016/j.envpol.2018.05.060>.

References

- Aharoni, C., Ungarish, M., 1977. Kinetics of activated chemisorption. Part 2.-Theoretical models. *J. Chem. Soc., Faraday Trans. 1* 73 (0), 456–464.
- Batchelli, S., Muller, F.L.L., Chang, K.-C., Lee, C.-L., 2010. Evidence for strong but dynamic iron–humic colloidal associations in humic-rich coastal waters. *Environ. Sci. Technol.* 44 (22), 8485–8490.
- Brookes, P.C., 1995. The use of microbial parameters in monitoring soil pollution by heavy metals. *Biol. Fertil. Soils* 19 (4), 269–279.
- Brose, D.A., James, B.R., 2013. Hexavalent chromium reduction by Tartaric acid and Isopropyl alcohol in mid-atlantic soils and the role of Mn(III,IV)(hydr)oxides. *Environ. Sci. Technol.* 47 (22), 12985–12991.
- Cao, C.-Y., Qu, J., Yan, W.-S., Zhu, J.-F., Wu, Z.-Y., Song, W.-G., 2012. Low-cost synthesis of flowerlike α -Fe₂O₃ nanostructures for heavy metal ion removal: adsorption property and mechanism. *Langmuir* 28 (9), 4573–4579.
- Chang, Y.-C., Chen, D.-H., 2005. Preparation and adsorption properties of mono-disperse chitosan-bound Fe₃O₄ magnetic nanoparticles for removal of Cu(II) ions. *J. Colloid Interface Sci.* 283 (2), 446–451.
- Freundlich, H., 1906. Over the adsorption in solution. *J. Phys. Chem.* 57, 385–470.
- Ge, Y., Schimel, J.P., Holden, P.A., 2011. Evidence for negative effects of TiO₂ and ZnO nanoparticles on soil bacterial communities. *Environ. Sci. Technol.* 45 (4), 1659–1664.
- Grossl, P.R., Eick, M., Sparks, D.L., Goldberg, S., Ainsworth, C.C., 1997. Arsenate and chromate retention mechanisms on goethite. 2. Kinetic evaluation using a pressure-jump relaxation technique. *Environ. Sci. Technol.* 31 (2), 321–326.
- Gu, B., Schmitt, J., Chen, Z., Liang, L., McCarthy, J.F., 1994. Adsorption and desorption of natural organic matter on iron oxide: mechanisms and models. *Environ. Sci. Technol.* 28 (1), 38–46.
- Gupta, V.K., Mittal, A., Gajbe, V., Mittal, J., 2006. Removal and recovery of the hazardous azo dye acid orange 7 through adsorption over waste materials: Bottom ash and de-oiled soy. *Ind. Eng. Chem. Res.* 45 (4), 1446–1453.
- He, Y.T., Wan, J., Tokunaga, T., 2008. Kinetic stability of hematite nanoparticles: the effect of particle sizes. *J. Nanoparticle Res.* 10 (2), 321–332.
- Hiraide, M., 1992. Heavy metals complexed with humic substances in fresh water. *Anal. Sci.* 8 (4), 453–459.
- Hu, J.-D., Zevi, Y., Kou, X.-M., Xiao, J., Wang, X.-J., Jin, Y., 2010. Effect of dissolved organic matter on the stability of magnetite nanoparticles under different pH and ionic strength conditions. *Sci. Total Environ.* 408 (16), 3477–3489.
- Huang, J., Wan, Q., 2009. Gas sensors based on semiconducting metal oxide one-dimensional nanostructures. *Sensors* 9 (12), 9903.
- Iglesias, A., López, R., Gondar, D., Antelo, J., Fiol, S., Arce, F., 2010. Adsorption of paraquat on goethite and humic acid-coated goethite. *J. Hazard Mater.* 183 (1–3), 664–668.
- Jiang, W., Cai, Q., Xu, W., Yang, M., Cai, Y., Dionysiou, D.D., O’Shea, K.E., 2014. Cr(VI) adsorption and reduction by humic acid coated on magnetite. *Environ. Sci. Technol.* 48 (14), 8078–8085.
- Kazakis, N., Kantiranis, N., Kalaitzidou, K., Kaprara, E., Mitrakas, M., Frei, R., Vargemzis, G., Vogiatzis, D., Zouboulis, A., Filippidis, A., 2018. Environmentally available hexavalent chromium in soils and sediments impacted by dispersed fly ash in Sarigkiol basin (Northern Greece). *Environ. Pollut.* 235, 632–641.
- Kendelewicz, T., Liu, P., Doyle, C.S., Brown Jr., G.E., 2000. Spectroscopic study of the reaction of aqueous Cr(VI) with Fe₃O₄ (111) surfaces. *Surf. Sci.* 469 (2–3), 144–163.
- Leita, L., Margon, A., Pastrello, A., Arçon, I., Contin, M., Mosetti, D., 2009. Soil humic acids may favour the persistence of hexavalent chromium in soil. *Environ. Pollut.* 157 (6), 1862–1866.
- Liu, J., Zhao, Z., Jiang, G., 2008. Coating Fe₃O₄ magnetic nanoparticles with humic acid for high efficient removal of heavy metals in water. *Environ. Sci. Technol.* 42 (18), 6949–6954.
- Lovley, D.R., Coates, J.D., Blunt-Harris, E.L., Phillips, E.J.P., Woodward, J.C., 1996. Humic substances as electron acceptors for microbial respiration. *Nature* 382 (6590), 445–448.
- MLR, E. a. The environmental protection department and the ministry of land and resources issued the national soil pollution condition investigation communique. http://www.mlr.gov.cn/xwdt/jrxw/201404/t20140417_1312998.htm.
- Mulvaney, P., Cooper, R., Grieser, F., Meisel, D., 1988. Charge trapping in the reductive dissolution of colloidal suspensions of iron(III) oxides. *Langmuir* 4 (5), 1206–1211.
- Nannipieri, P., Ascher, J., Ceccherini, M.T., Landi, L., Pietramellara, G., Renella, G., 2003. Microbial diversity and soil functions. *Eur. J. Soil Sci.* 54 (4), 655–670.
- Nethaji, S., Sivasamy, A., Mandal, A.B., 2013. Preparation and characterization of corn cob activated carbon coated with nano-sized magnetite particles for the removal of Cr(VI). *Bioresour. Technol.* 134, 94–100.
- Niwas, R., Gupta, U., Khan, A.A., Varshney, K.G., 2000. The adsorption of phosphamidon on the surface of styrene supported zirconium (IV) ditionstophosphate: a thermodynamic study. *Colloids Surf. Physicochem. Eng. Aspects* 164 (2–3), 115–119.
- Qiu, H., Lv, L., Pan, B.-c., Zhang, Q.-j., Zhang, W.-m., Zhang, Q.-x., 2009. Critical review in adsorption kinetic models. *J. Zhejiang Univ. - Sci. A* 10 (5), 716–724.
- Sing, K.S.W., Everett, D.H., Haul, R.A.W., Moscou, L., Pierotti, R.A., Rouquerol, J., Siemieniowska, T., 1985. Reporting physisorption data for gas solid systems with special reference to the determination of surface-area and porosity (recommendations 1984). *Pure Appl. Chem.* 57 (4), 603–619.
- Stevenson, F.J., 1994. *Humus Chemistry: Genesis, Composition, Reactions*. John Wiley & Sons.
- Tang, L., Yang, G., Zeng, G., Cai, Y., Li, S., Zhou, Y., Pang, Y., Liu, Y., Zhang, Y., Luna, B., 2014. Synergistic effect of iron doped ordered mesoporous carbon on adsorption-coupled reduction of hexavalent chromium and the relative mechanism study. *Chem. Eng. J.* 239, 114–122.
- Tippling, E., Rey-Castro, C., Bryan, S.E., Hamilton-Taylor, J., 2002. Al(III) and Fe(III) binding by humic substances in freshwaters, and implications for trace metal speciation. *Geochem. Cosmochim. Acta* 66 (18), 3211–3224.
- Weng, C.-H., Lin, Y.-T., Tzeng, T.-W., 2009. Removal of methylene blue from aqueous solution by adsorption onto pineapple leaf powder. *J. Hazard Mater.* 170 (1), 417–424.
- Wu, Z., Zhong, H., Yuan, X., Wang, H., Wang, L., Chen, X., Zeng, G., Wu, Y., 2014. Adsorptive removal of methylene blue by rhamnolipid-functionalized graphene oxide from wastewater. *Water Res.* 67 (0), 330–344.
- Yang, Z.H., Xiao, Y., Zeng, G.M., Xu, Z.Y., Liu, Y.S., 2007. Comparison of methods for total community DNA extraction and purification from compost. *Appl. Microbiol. Biotechnol.* 74 (4), 918–925.
- Yang, G., Tang, L., Cai, Y., Zeng, G., Guo, P., Chen, G., Zhou, Y., Tang, J., Chen, J., Xiong, W., 2014. Effective removal of Cr(VI) through adsorption and reduction by magnetic mesoporous carbon incorporated with polyaniline. *RSC Adv.* 4 (102), 58362–58371.
- Zachara, J.M., Girvin, D.C., Schmidt, R.L., Resch, C.T., 1987. Chromate adsorption on amorphous iron oxyhydroxide in the presence of major groundwater ions. *Environ. Sci. Technol.* 21 (6), 589–594.
- Zhang, J., Chen, L., Yin, H., Jin, S., Liu, F., Chen, H., 2017. Mechanism study of humic acid functional groups for Cr(VI) retention: two-dimensional FTIR and ¹³C CP/MAS NMR correlation spectroscopic analysis. *Environ. Pollut.* 225, 86–92.
- Zheng, Y., Wang, C., Zheng, Z., Che, J., Xiao, Y., Yang, Z., Zhao, F., 2014. Ameliorating acidic soil using bioelectrochemistry systems. *RSC Adv.* 4 (107), 62544–62549.
- Zheng, Y., Xiao, Y., Yang, Z.-H., Wu, S., Xu, H.-J., Liang, F.-Y., Zhao, F., 2014. The bacterial communities of bioelectrochemical systems associated with the sulfate removal under different pHs. *Process Biochem.* 49 (8), 1345–1351.